

Lateral Energy Confinement of Multi-layered SAW Resonator Employing Low-cut Lithium Tantalate

Yiwen He¹, Yu-Po Wong², Qi Liang¹, Ting Wu¹, Jingfu Bao^{1†}, and Ken-ya Hashimoto^{1,2}
(¹Univ. Elect. Sci. Technol. China; ²Chiba Univ.)

1. Introduction

Recently, I.H.P. SAW with multi-layered structure has aroused appreciable interest owing to its small TCF and high Q values with incredible acoustic energy confinement [1] [2].

Despite the fact that energy can be well confined to the surface, there still remains energy leakage through the busbar and causes excess loss. For its ultimate reduction, gaps between electrode finger tips and busbars must be designed properly. For $42^\circ\text{YX-LiTaO}_3$ (LT) including I.H.P. SAW, dummy electrodes (dummies) are applied to suppress strong scattering loss [3]. However, the energy confinement provided by busbar cannot cover the entire passband. Huck, et al, proposed to use gap short structure (GSS) [4], instead of dummies, for further suppression. This year, the author's group proposed the double busbar configuration [5]. The results exhibited both good energy confinement and transverse mode suppression on I.H.P SAW when the piston mode design is also applied to the configuration.

Since low-cut LT has larger electromechanical coupling factor than 42-LT, it seems promising for application to wide band filters provided that well energy confinement and spurious mode suppression can be achieved.

This paper discusses applicability of the double busbar configuration to the multi-layered SAW configuration on 20°YX-LT for better energy confinement. The effect of piston mode to suppress transverse modes has also been studied. Periodic 3D FEM simulations powered by HCT are applied to validate the merits of double busbar design [6].

2. Energy confinement for different designs

Fig. 1 shows one period of the electrode patterns discussed in this paper. The perfect matching layers (PMLs) are given to the side edges, while the periodic boundary conditions are applied to the top and bottom boundaries. Fig. 1 (a) and (b) show the conventional ones without and with dummy electrodes, respectively, and Fig.1(c) shows the double-busbar structure proposed in [5]. A layered configuration of $20^\circ\text{YX-LT}/\text{SiO}_2/\text{Si}$ is employed as the substrate. In the following calculation, LT, SiO_2 and Al electrode thicknesses are chosen as $0.736 \mu\text{m}$, $0.6 \mu\text{m}$, and $0.09p_1$, respectively, where p_1 is the

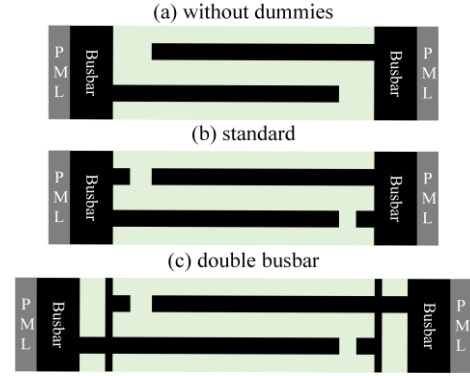


Fig.1 Top view of the three designs of the multi-layered SAW on 20°YX-LT : (a) without dummies, (b) standard, (c) double busbar.

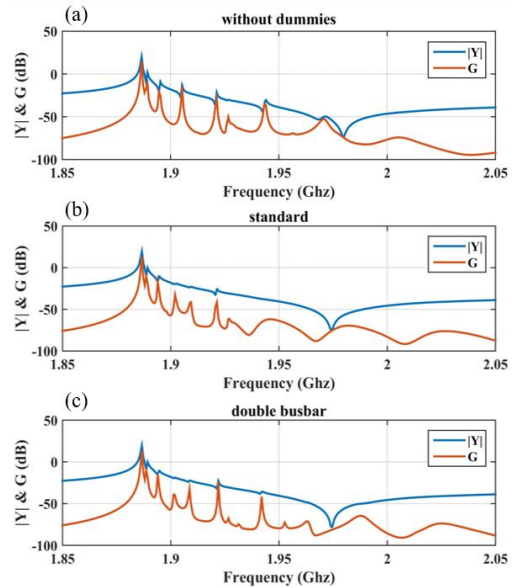


Fig.2 Calculated admittance (Y) and conductance (G) from (a) without dummies design, (b) standard design, (c) double busbar design.

IDT periodicity ($2 \mu\text{m}$), and the gap distance is set at $0.2p_1$. Since only tiny material loss is added in the FEM model, losses appearing in the following simulations are mainly due to energy leakage through busbars and scattering to bulk waves.

Fig. 2 shows admittance (Y) and conductance (G) calculated by periodic 3D FEM. When the dummies are not given, the conductance levels are elevated upward at frequencies above 1.925 GHz (see Fig. 2(a)). This is caused by the scattering at the gap region [3][5].

On the other hand, when the dummies are given,

[†]baojingfu@uestc.edu.cn

the elevation was suppressed (see Fig. 2(b)). Note that shorter gap length gives better performance, similar to 42°YX-LT [3]. Resonance peaks above 1.925 GHz are not steep. This means the transverse modes are leaky in the frequency range.

In contrast, when the double busbar is applied, resonance peaks are steep until 1.965 GHz.

Fig. 3 shows variation of the frequency dependence of Bode Q [7] with the electrode pattern design. It is seen that the double busbar gives the best Bode Q for the frequency range from 1.925 GHz to 1.965 GHz without deterioration of the Bode Q in other frequencies.

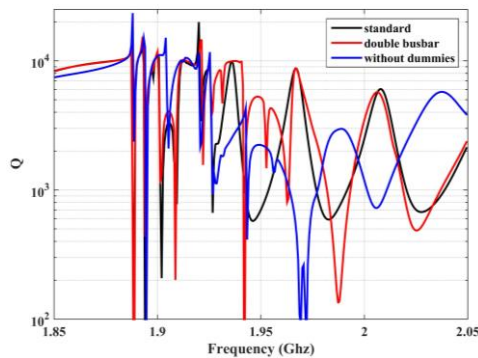


Fig.3 Variation of Bode Q with the electrode patterns on multilayered configuration on 20°YX-LT.

Some energy leakage can still be seen above 1.965 GHz. This is due to insufficient SAW velocity difference between electrode and gap regions [5]. This problem might be solved by redesigning the whole device configuration.

3. Piston mode for spurious mode suppression

Next, the piston mode design is applied to the double busbar design for the transverse mode suppression.

Fig.4 shows Y and G of double busbar design with piston mode operation. And the top view of basic configuration (single period) is shown in the inset. The transverse modes are suppressed in some extent.

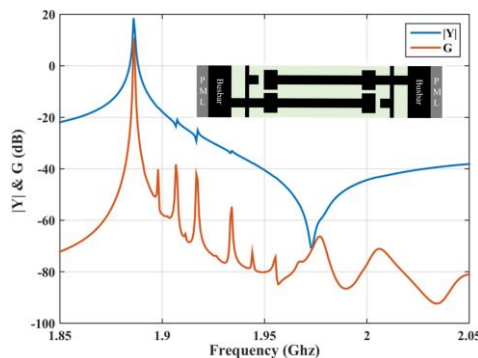


Fig.4 Calculated admittance (Y) and conductance (G) double busbar design with piston mode design.

Fig. 5 shows the Bode Q for this case. No apparent degradation is seen when this figure is compared with Fig. 3.

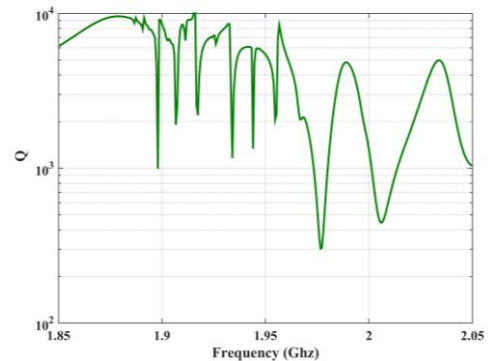


Fig.5 Bode Q when the piston mode design is applied to the double busbar configuration.

4. Conclusion

This paper discussed the energy confinement of three different designs in multi-layered SAW resonators employing low-cut LT.

It is found that dummies are necessary for scattering suppression also in 20°YX-LT and narrow gap is preferable. Besides, double busbar can provide wider energy confinement while realize the electrode connection for dummies to create an extra gap between dummies and busbar. Furthermore, piston mode can realize better spurious suppression.

The next target is further improvement of energy confinement and transverse mode suppression.

Acknowledgment

This work was supported by the grant from the National Natural Science Foundation of China and the China Academy of Engineering Physics Grant (Project No. U1430102).

References

- [1]. T. Takai, et al, Proc. IEEE Ultrason. Symp. (2016) 10.1109/ULTSYM.2016.7728455.
- [2] T. Takai, et al, IEEE Transactions on Ultrasonics, Ferroelectrics, and Frequency Control, **64**, 9 (2017) pp. 1382-1389.
- [3] M. Solal, et al, IEEE Transactions on Ultrasonics, Ferroelectrics, and Frequency Control, **60**, 9 (2013) pp. 2404-2413.
- [4] C. Huck, International Patent WO 2020/120153. (2020)
- [5] Y. P. Wong, et al, to be published in Proc. IEEE Ultrason. Symp. (2021)
- [6] X. Li, et al, IEEE Transactions on Ultrasonics, Ferroelectrics, and Frequency Control, **66**, 12 (2019) pp.1920-1926.
- [7] D. A. Feld, et al, Proc. IEEE Ultrason. Symp. (2008) pp. 431-436.